Numerical Realization of Mathematical Model of Transfer and Diffusion of Impurity in the Atmosphere Interface

Allayarbek Aydosov[1], Nurgali Zaurbekov[2], Nurbike Zaurbekova[3], Gulzat Zaurbekova[4], Galym Aydosov[5], Kairat Imanbayev[6], Sapargali Zaurbekov[7]

Abstract

The aim of research carried out in this paper is the application of mathematical modeling capabilities for environmental monitoring, through the development of models and algorithms for numerical simulation of the spread of harmful impurities in the atmosphere. Achieving this goal is due to the decision of a complex of interrelated problems:

1) the mathematical modeling of the transport of harmful impurities in the atmosphere;

2) implementation of a mathematical model.

Keywords: mathematical model; diffusion of impurities; boundary layer; atmosphere; atmospheric stability; real object.

Introduction

Population growth and industrial production are inextricably linked to energy consumption. This, in turn, stimulates the development of the energy producing industries, which leads, in particular, to an increase in consumption of natural resources, the construction of new large power plants (thermal, nuclear and hydroelectric power plants), and the introduction of energy saving technologies. Energy consumption is growing in the world.

Energy development is associated with intense exposure to energy producing industries to the environment.

First of all, this effect appears on the stage of mining, in particular, organic and nuclear fuel needed for the operation of thermal and nuclear power plants. When operating the power plants consumed a large amount of water used in the process cycle power plants. There develops engineering, aircraft, and other energy-intensive industries. The increase in population and industrial development require intensive energy development.

Furthermore, during the operation of power objects in the environment, it receives a significant amount of pollutants different physical nature. This is primarily different chemical substances and compounds, radio-nuclides and thermal emissions and discharges associated with the operation of cooling systems. Enters the atmosphere and bodies of water, pollutants have a negative impact on the functioning of ecological systems and human health.

The environmental situation in the areas where power plants are largely determined by the nature of the polluting emissions of substances into the atmosphere of these enterprises. The level of exposure received by the atmosphere of polluting

[1]PhD, Professor, Almaty Technological University, 50052, Republic of Kazakhstan, Almaty, Tole bi str., 100

[2]PhD, Professor, Almaty Technological University, 50052, Republic of Kazakhstan, Almaty, Tole bi str., 100, agu_nurgali@mail.ru

[3]PhD, Satpayev Kazakh National Technical University, 050013, Republic of Kazakhstan, Almaty 22a, Satpaev str., nurbike_zh@mail.ru

[4]Doctoral, Al-Farabi Kazakh National University, 050040, Republic of Kazakhstan, Almaty, 71 al-Farabi Ave., guzzzya_92@mail.ru

[5]PhD, Professor, Al-Farabi Kazakh National University, 050040, Republic of Kazakhstan, Almaty, 71 al-Farabi Ave., galym_a@mail.ru

[6]PhD, Almaty Technological University, 50052, Republic of Kazakhstan, Almaty, Tole bi str., 100, k_imanbayev@mail.ru

[7]L.N.Gumilyov Eurasian National University, 010008, Astana, Republic of Kazakhstan, Satpayev Str., 2, sapar_z@rambler.ru

substances, depending on their physical nature, power output and specific weather conditions of the region. Among the pollutants of various physical natures, a special place is occupied by chemical emissions, emissions of radionuclides, as well as heat emissions associated with entering the atmosphere of a large amount of heat and moisture.

Since a large radiochemical and thermodynamic activity of anthropogenic emissions cannot be regarded as conservative impurities, and is therefore required to consider the mechanism of interaction of these impurities from the atmosphere and other objects in the surrounding environment in detail. Exposure to a variety of sources on the environment was considered by some researchers, however, these studies have focused mainly single source and not taken into account the specific climatic conditions of the Central Asian region. Research propagation conditions in the environment of anthropogenic emissions from the power plants, the mechanism of their effects on human health and the environment, as well as the modeling of this impact in order to make management decisions examined now is not enough, and for industrial enterprises located on the territory of Kazakhstan, virtually not conducted. That is why the problem is considered in this paper is relevant and practically important.

The authors determined the propagation conditions in the atmosphere of anthropogenic emissions from power plants in the territory of Kazakhstan, and quantification of the impact on public health and the environment based on the model of the diffusion of harmful impurities.

It is usually assumed that the wind field is spatially uniform and turbulence is uniform in the field. In these cases, use empirical models such as Gaussian, satisfactorily describe the scattering process. However, the possibility of such models for describing the spread of impurities in the turbulent boundary layer to the spatial dimensions of the order of 100 km, is limited. This is due to the complex nature of meteorological processes in a limited area, depending on orographic irregularities, the variability of the characteristics of the turbulent atmosphere, non-uniform thickness of the mixed layer, etc. In such cases, cannot take into account the spatial inhomogeneity of the velocity field changes and atmospheric turbulence. Currently, the greatest success in the modeling of the transport processes and transport of contaminants in complex meteorological and orographic conditions obtained on the basis of the use of three-dimensional grid models. In this paper, we consider the description of one of these models, its numerical implementation and illustrated by the range of possible practical applications.

Atmospheric impurities are multi-media and the various components that communicate with the atmosphere and each other. As a result of chemical reactions can occur, new substances are not contained in the original sources of the substances emitted.

Using the equation of conservation of mass for the impurities in the air, which describes the transport, turbulent diffusion, chemical reaction, deposition and release of pollutants, based on the model described in (Aidosov A.A., Aidosov G.A., Zaurbekov N.S., 2010) we obtain the equation averaged over the ensemble of concentrations:

$$\frac{\partial \tilde{N}_i}{\partial t} = -U\frac{\partial C_i}{\partial x} + V\frac{\partial C_i}{\partial y} + W\frac{\partial C_i}{\partial z} + \frac{\partial}{\partial x}\left(k_H \frac{\partial C_i}{\partial x}\right) + \frac{\partial}{\partial y}\left(k_H \frac{\partial C_i}{\partial y}\right) + \frac{\partial}{\partial z}\left(k_z \frac{\partial C_i}{\partial z}\right) + R_i + Q_i,$$

(i=1, m), (1) (3.56)

where: m– total impurities ingredients; C_i – concentration of i-th impurities; U, V and W – the components of the velocity vector; t– время; R_i– the production rate of i-th impurities, and by chemical reactions; Q_i– known function describing sources of emissions and power of i-th impurities. Function R_i– determined using appropriate chemical kinetics relationships form:

$$R_i = -\left(\sum_j d_i^j \prod_{k \neq i} C_k\right) C_i + \sum_l \left(P_i^l \prod_m C_m\right), \qquad (2)$$

where: d_i^j – absorption coefficient of i-th reaction for impurities j; P_i^l – скорость производства i-ой примеси для реакции l; C_k, C_m– ингредиенты impurities, respectively involved in the reactions j and l.

Formally, the equation (1) of the parabolic type, but in many situations meteorological transfer of impurities in a horizontal plane relative to

dominate diffusion and this leads to a substantial hyperbolic of the system which greatly complicates the construction of adequate numerical algorithms. Significant difficulties also arise in the numerical solution of the equations of chemical kinetics type (2), as the chemical reactions can participate impurities with a lifetime from 10^{-7} to 10^{5} seconds, and this leads to the "rigidity" of the system of ordinary differential equations with the right-hand side of the form (2).

The boundary conditions for the problem (2) shall be made in the following form. The upper boundary of the atmospheric boundary layer height *H*- conditions for the absence of the impurity from the bottom, ie, $\left\{k_z \frac{\partial C_i}{\partial z}\right\}_{z=H}$. On the bottom of the boundary layer is determined by the condition of deposited impurities reacting with the underlying surface and is defined as $\left\{k_z \frac{\partial C_i}{\partial z} = V_g^i C_i\right\}_{z=0}$, where V_g^i – the deposition rate of i-th impurity, determined by using special techniques (Penenko V.V., Aloyan A.E. et al., 1985). At the side boundaries at $x=X_w$ or $x=X_E$ and at $y=Y_S$ or $y=Y_N$, $X_E X_w$, Y_S, Y_N – western, eastern, southern and northern boundaries of the modeled area, respectively, the boundary conditions are determined depending on the input flow in the area. On the border of the "input" put the condition $UC - k_H \frac{\partial C_i}{\partial x} = UC_i^0$, on the "output" $-k_H \frac{\partial C_i}{\partial x} = 0$, where is for being specific is considered $x=X_w$ or $x=X_E$, a δ_i^0 – known function describing the change in concentration of the i-th impurity on the front edge. The initial conditions at the $t=0$ usually assumed to be zero because very difficult to determine the initial concentration at all points of the grid area due to the sparsity and irregularities Observing System for air quality status.

The expression for the vertical turbulent exchange coefficient is shown in Table 1.

Table 1. Vertical turbulent exchange

Stability	$k_z = KU_* Z/(0.74 + 4.77/L)$
Normal conditions	$k_z = KU_* Z l^{\frac{-4z}{H}}$
Instability	$k_z = \begin{cases} w_* Z_i \left[2.5\left(\frac{KZ}{Z_i}\right)^{\frac{4}{3}}\left(1-\frac{15Z}{L}\right)^{\frac{1}{4}}\right], 0 \le \frac{Z}{Z_i} \le 0.5; \\ w_* Z_i \left[2\exp\left(6-\frac{10Z}{L}\right)\right], 0.05 \le Z \le 1.1; \\ w_* Z_i 0.001, \quad \frac{Z}{Z_i} \ge 1.1 \end{cases}$

Determination of the coefficient of horizontal turbulent exchange is currently considerable difficulties. However, as authors have already noted, in many meteorological situations impurity transport by diffusion is much less than by advection. In these cases, the dominant role is played by "artificial" viscosity, resulting discrete approximation is hyperbolic terms in the equations and the distribution of the impurity concentration is insensitive to the choice of competitive values k_H.

Materials and Methods

Numerical realization of the model transfer and diffusion of impurities in the atmospheric boundary layer.

The analysis of the main methods of modeling of pollution spreading in the air indicates the need to use for this purpose a broad class of numerical models. And in most cases, these models are based on the use of atmospheric turbulent diffusion equation (Yaglom A.M., 1972), taking into account the main features of the simulated weather situations.

Consider a numerical model of the transfer and diffusion of impurities in the boundary layer of the atmosphere with the characteristic horizontal scale of about 100-200 km on a background of local atmospheric processes. All required fields of meteorological and turbulent characteristics of hydrodynamics define the model described in (Aidosov A.A., Aidosov G.A., Zaurbekov N.S., 2010). For the numerical integration of the splitting method to the system of four partial differential equations split into a three-dimensional system of equations in the variables (x, t), (y, t), and (z, t). Each of these systems is integrated consecutively at each time step, and the resultant solution at the end of the cycle approximates the original system of equations (1). Thus, the problem reduces to the integration of the following systems:

$$\frac{\partial C_i}{\partial t} + U\frac{\partial C_i}{\partial x} = \frac{\partial}{\partial x}\left(k_H \frac{\partial C_i}{\partial x}\right); \quad (3)$$

$$\frac{\partial C_i}{\partial t} + V\frac{\partial C_i}{\partial y} = \frac{\partial}{\partial y}\left(k_H \frac{\partial C_i}{\partial y}\right); \quad (4)$$

$$\frac{\partial C_i}{\partial t} + W\frac{\partial C_i}{\partial z} = \frac{\partial}{\partial z}\left(k_z \frac{\partial C_i}{\partial z}\right) + R_i + Q_i. \quad (5)$$

If to introduce the notation T_x, T_y и T_z for numerical approximations of the operators of transport of impurities in the directions *X*, *Y*, and *Z* respectively, T_c for chemical transformation operator and the emission sources, the total solution can be obtained in the form of:

$$C^{n+1} = T_x T_y T_z T_c T_S(\alpha\Delta t) T_z T_x T_y \left[C^{n-1}\right], \quad (6)$$

where: Δt – a step by time; n – the current number of the sacrificial layer.

Operators T_x, T_y, and T_z are splitting into the diffusive and advective components, i.e. $T_x=(T_x)_a(T_x)_d$, $T_y=(T_y)_a(T_y)_d$, $T_z=(T_z)_a(T_z)_d$.

Consider separate solutions for each step of the three main basic functional equations corresponding advection, diffusion, chemical transformation, by which, according to (6), the resulting solution is determined at time $n*\Delta t$.

a) Solution of advection equation is based on the use of explicit difference scheme with second-order approximation which has the property of conservatism for the masses. This scheme is as follows:

$$(T_x) = [C_{ikl}] = \frac{\left[F_{i-\frac{1}{2},k,l} - F_{i+\frac{1}{2},k,l}\right]}{\Delta t}, \quad (7)$$

where

$$F_{i-\frac{1}{2},k,l} = \frac{\Delta t\left[\frac{U_{i-\frac{1}{2},k,l}\left(C_{i-1,k,l}+C_{i,k,l}\right)}{2}\right]}{\frac{1}{2}(\Delta x_i + \Delta x_{i-1})} - \frac{\frac{1}{2}\Delta t^2\left[\frac{U^2_{i-\frac{1}{2},k,l}\left(C_{i,k,l}-C_{i-1,k,l}\right)}{\Delta x_{i-1}}\right]}{\frac{1}{2}(\Delta x_i + \Delta x_{i-1})}; \quad (8)$$

$$F_{i+\frac{1}{2},k,l} = \frac{\Delta t\left[\frac{U_{i+\frac{1}{2},k,l}\left(C_{i+1,k,l}+C_{i,k,l}\right)}{2}\right]}{\frac{1}{2}(\Delta x_i + \Delta x_{i-1})} + \frac{\frac{1}{2}\Delta t^2\left[\frac{U^2_{i+\frac{1}{2},k,l}\left(C_{i,k,l}-C_{i+1,k,l}\right)}{\Delta x_i}\right]}{\frac{1}{2}(\Delta x_i + \Delta x_{i-1})}. \quad (9)$$

To prevent significant technical errors and blurring the "peak" concentrations, as well as preserving the positive values of Cikl variables were used the flow adjustment:

$$F_{i-\frac{1}{2},k,l} = \begin{cases} C_{i,k,l}, if U_{i-\frac{1}{2},k,l} \le 0, \quad C_{i,k,l} < F_{i-\frac{1}{2},k,l} \\ C_{i-1,k,l}, if U_{i-\frac{1}{2},k,l} > 0, \quad C_{i-1,k,l} < F_{i-\frac{1}{2},k,l} \end{cases}; \quad (3.66)$$

$$F_{i+\frac{1}{2},k,l} = \begin{cases} C_{i,k,l}, if U_{i+\frac{1}{2},k,l} \ge 0, \quad C_{i,k,l} < F_{i+\frac{1}{2},k,l} \\ C_{i+1,k,l}, if U_{i+\frac{1}{2},k,l} < 0, \quad C_{i+1,k,l} < F_{i+\frac{1}{2},k,l} \end{cases}. \quad (3.67)$$

Similar relations can be obtained for components *y*, *Z*:

b) Different schemes for the solution of the diffusion equation are constructed according to the coordinate directions. The horizontal plane is

dominated by advection, so there can be used the usual three-point explicit scheme:

$$(T_x)=\left[k_{H\,i+\frac{1}{2}}\left(C_{i+1,kl}-C_{ikl}\right)\Delta x_i-k_{H\,i-\frac{1}{2}}\right]\left(C_{ikl}-C_{i-1\,kl}\right)\Delta x_i \quad . \quad (3.68)$$

For directions Z, in order to reduce restrictions on the choice of the implicit Crank-Nicholson scheme.

c) The chemical transformation step is reduced to solving the interval $\alpha\Delta t$ in each grid point of the simulated field system of ordinary differential equations of the form:

$$\frac{\partial C_i}{\partial t}=R_i, \quad i=\overline{1,m} \quad , \quad (3.69)$$

where R_i is determined by depending on the type (3.57)

Due to the marked rigidity of the system (3.69), semi-implicit methods should be used for the solution. One of the simplest methods of this class is implemented as follows. Let the concentration of impurities (excluding *i*) are known (from the previous step, or, or has already been calculated in the current step). Then the solution of (3.69) can be approximated by the formula:

$$C_i\big|_{t+\Delta t^{|}}=\left.\frac{P_i}{D_i}\right|_t+\left(C_i-\left.\frac{P_i}{D_i}\right)\right|_t e^{-D_i\Delta t^{|}} \quad , \quad (3.70)$$

based on the ratio:

$$\frac{\partial C_i}{\partial t}=-D_iC_i+P_i \ , \quad \text{where}$$
$$D_i=\sum_j d_i^j\prod_{k\neq i}C_k, \qquad P_i=\sum_l P_i^l\prod C_m, \quad i=1,m. \quad (3.71)$$

The proposed algorithm is based on the numerical integration of the division involved in the chemical reactions of impurities in the two groups. The first group (possibly, empty) make short-type impurity *OH*, H_2O_2. The other group consists of the remaining long-lived impurities (SO_2, CO_2, etc.) To determine the concentrations of impurities Group uses a system of algebraic equations obtained from the pseudo-steady-state approximation of the corresponding right-hand sides in (3.71):

$$C_i=\frac{P_i}{D_i}=\frac{\sum_l P_i^l\prod_{m\in I_1}\overline{C_m}\prod_{n\in I_2}C_n}{\sum_j d_i^j\prod_{k\neq i}\overline{C_k}\prod_{n\in I_2}C_n} \quad , \quad (3.72)$$

where I_1, I_2 – set of indices corresponding to a short-lived and long-lived impurities nadcherkom designated set the value of the impurity concentration of the first group. Concentrations of contaminants related to the number of long-lived, and continue to be calculated using the formula (3.70).

The accuracy depends on the integration $\Delta t^{|}$ and constants of chemical reactions (3.71). For slow-reacting in the air impurities can be used fairly large time step, but it will be much less if some impurities are responsive (typically $\Delta t^{|}$=0.1-5 minutes, and Δt=5-10 minutes).

One of the main difficulties encountered when using numerical grid models, is the transition from the description of the characteristics of impurity sources with a local subgrid scale the mesh to their submission. In the case where the initial flame emission dimensions comparable to the size of the grid cell corresponding to the description of the net source of these emissions is not difficult and is fairly accurate. Therefore, you can use the following procedure to parameterize point sources. We calculate on the basis of mesh sizes Δx , Δy, Δz and diffusion rates, the time interval T during which the magnitude of the width of the plume becomes deliquescent comparable scale grid:

$$T=\min\left\{\frac{\Delta x^2}{kH},\frac{\Delta y^2}{kH},\frac{\Delta z^2}{kH}\right\}. \quad (3.73)$$

Now, using the information on the velocity vector $\vec{v}$, define the new position of the center of the torch according to the formula:

$$\vec{v} = \vec{v_0} + \vec{VT}, \qquad (3.74)$$

where $\vec{v}$ – the initial position of the source and the corresponding nodes of the grid which can be taken in the numerical model for the sources of emissions of impurities.

The geometric height of the source H_s usually always lower than the actual height of the release, which is called the effective height of the temperature difference at the mouth of the pipe and in the surrounding air. Determination of the additional height of the flame rise above the pipe ΔH is a complicated task.

The most common here is the approach proposed by Berland (3.36), where ΔH is determined by the formula:

$$\Delta H = 24\left(\frac{F}{U^3}\right)^{\frac{3}{5}}\left(H_s + 200\frac{F}{U^3}\right)^{\frac{2}{5}}, \qquad (3.75)$$

for convective and neutral conditions:

$$\Delta H = 2.6\left(\frac{F}{US}\right)^{\frac{1}{3}}, \qquad (3.76)$$

for stable conditions. Here, F – heat flow of smoke emissions, U - the average wind speed, $S = \left(\frac{g}{T_A}\right)j$, j – potential temperature gradient; T_A – ambient temperature.

Discussion and Results

An illustrative example of a numerical calculation model of transport and diffusion of impurities in the atmospheric boundary layer and the construction of geo-environmental maps based on orographic terrain on the example of the Karachaganak oil and gas field.

Consider the calculation of results obtained using the developed numerical model of impurity propagation model for the next situation. In area X=Y=70 km, H=1700 m there is a source of passive impurity at the height H_s=250m at X=Y=0, Δx=Δy=4 km, Δz=50m at $z \le 200$m, Δz=200m at $z > 200$m, k_H=200m^2/s, U=5m/s, $v = w = 0$. The time integration was carried out in the interval of 24 hours. Figure 3.1 shows the results of the calculation across the average concentration integrated over wind C^y, normalized by the size $\frac{Q}{HU}$, where Q – power of the emission source. Distribution of impurities corresponds to the steady state. The figure analysis shows that near the source of the plume axis (ie, the maximum concentration line) descends and reaches the underlying surface. This phenomenon is confirmed by the data of numerous observations.

In particular, the classification of the atmospheric stability which determines the intensity of the turbulent diffusion is given using standard Raksvill-Gifford techniques.

By this method, depending on the wind velocity, time of day, the solar insolation and temperature gradient in the boundary layer of the atmosphere (BLA) are determined by six classes of stability (A, B, C, D, F), from A (maximum instability) and up to F (highest resistance).

Wind speed, as already noted, has a horizontal uniformity and specified using a simple model of the Ekman boundary layer. The intensity of the turbulent diffusion of height of boundary layer in the atmosphere was set using parameter of stability in the surface layer of the atmosphere L and a dynamic rate as in (Yaglom A.M., 1972; Godish Th., Davis W.T., Fu J.S., 2014). Definition L and u was carried out according to the approach where the specific values of these parameters is selected (for each class of stability) according to the known wind speed near the Earth's surface and the underlying surface roughness parameter z_0.

The strength of the wind in the BLA was determined by the power law:

$$|u| = u_r\left(z/z_r\right)^p,$$

where: p – the exponent-dependent z^0 and the class of stability; u_r – the known value of the surface wind at the height of z^r.

The rotation angle of the velocity vector in BLA (by Ekman model) is given by:

$$\alpha = \frac{\sin(z_q)}{\left(\exp(z_q) - \cos(z_q)\right)},$$

where $z_q = z\sqrt{\frac{kf}{20k_1}}$; k– Karman parametr 45; f– Coriolis parameter; k_1– the coefficient of vertical height on the exchange $|L|$.

In addition, these models also external to the PSA were used meteoparameters: h– the height of the atmospheric boundary layer; z_n – the height of BLA; α_g – wind direction in the selected coordinate system. Used values of these meteorological parameters and roughness parameters are presented in Table 3.2.

Table 3.2. The value of the external parameters

Meteosituation type	H	z^0	z_n	α_g	z^r	u_r
Convective conditions	10	0,1	600	10^0	8	3
Steady conditions	50	0,1	1500	-30^0	8	2

Given the gravity of the orography ground (earth surface roughness), the moisture balance in the atmosphere, the heat influx, including radiation heat flow, heterogeneity atmospheric environments unsaturated (rich) atmosphere in the presence of condensation, vertical movement in a cloudy atmosphere, and also taking into account the front surface using a numerical model of a baroclinic atmosphere described in the second section. The diagnostic system is solved for the intermediate points on the horizontal grid schemes of Marchuk by a conventional sweep. In general, this problem is reduced to the form (3.17) - (3.23) with the initial (3.24) - (3.24a) and boundary (3.25) - (3.27) conditions. The numerical values of meteorological parameters (temperature, wind speed, pressure, etc.) are used for the numerical solution of equations (3.64). The boundary conditions for the problem (3.64) as follows: the upper boundary layer of the atmosphere height H - condition for the absence of impurities from the bottom, at the lower boundary conditions are determined by the interaction of impurities deposited and the underlying surface and is given in the form n 3.8.1. At the side boundaries (western, eastern, southern, northern) boundary conditions are determined depending on the input flow in the area, and the initial conditions are assumed to be zero. In view of section 1 of the data, the following geo-ecological maps for the Karachaganak oil and gas condensate deposit.

Geo-environmental map is a transfer of harmful impurities in convective conditions. Distribution of impurities such as SO_2 and NO_2 in convective atmospheric conditions is devoted to Figures 3.1-3.12. These figures show the contours of concentration SO_2 and NO_2 (in fractions of maximum permissible concentration) at three levels of adjustment for the time corresponding to a complete purging of the deposit area. This time is approximately equal to $40000/u_r$ seconds, where u_r– surface air velocity in advance for this calculation option. And it usually corresponds to the period of time when the spread of contaminants becomes steady character. In a series of calculations (Figures 3.6-3.12) wind speed is increased by half compared with the calculation of the options presented in Figures 3.1-3.5. It can be seen that the increase in wind speed contributes to more intensive removal of impurities from the area of the deposit.

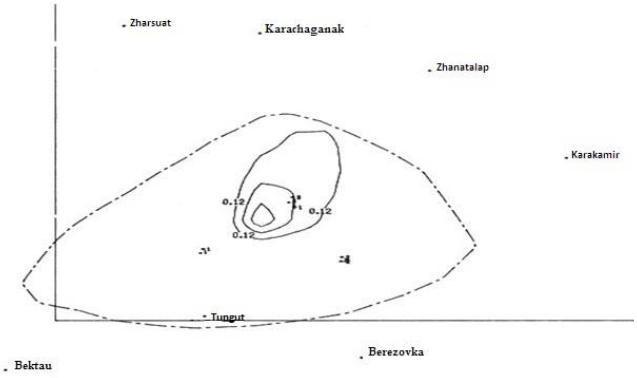

Fig. 3.1. Isolines of CO_2 concentration in the MAC shares at the lower boundary of the surface layer. Max CO_2 – 0.47

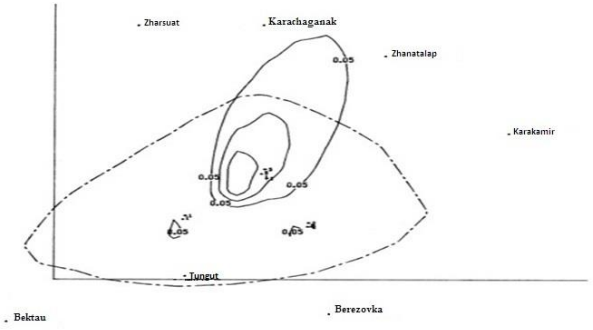

Fig. 3.2. Isolines of CO_2 concentration in the MAC shares at an altitude of 650 m.
Max CO_2 – 0.22

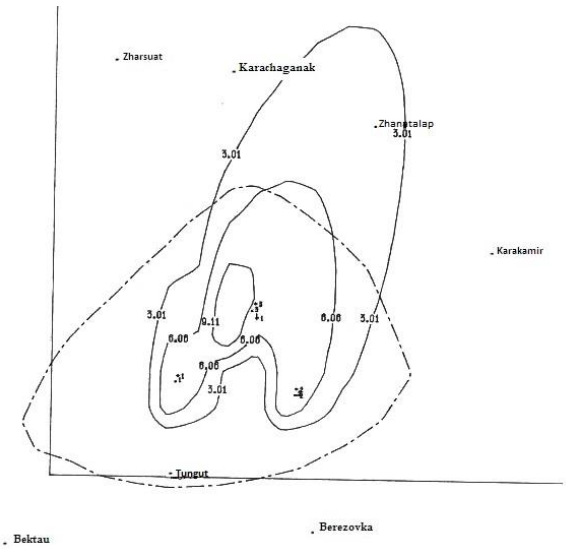

Fig. 3.3. Isolines of NO_2 concentrations in MAC shares at an altitude of 50 m.
Max NO_2 –12.16

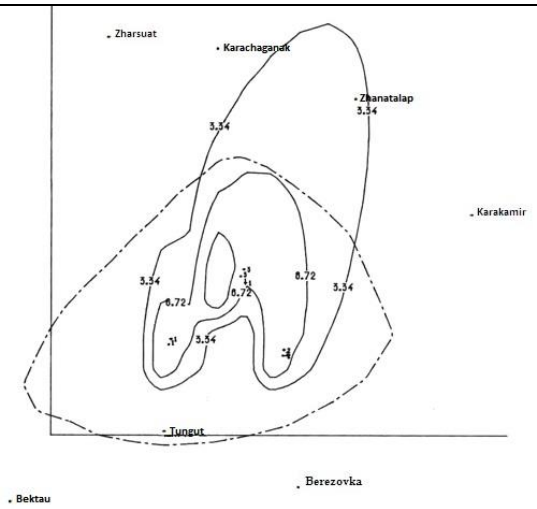

Fig. 3.4. Isolines of NO_2 concentrations in MAC shares at an altitude of 250 m.
Max NO_2 – 13.47

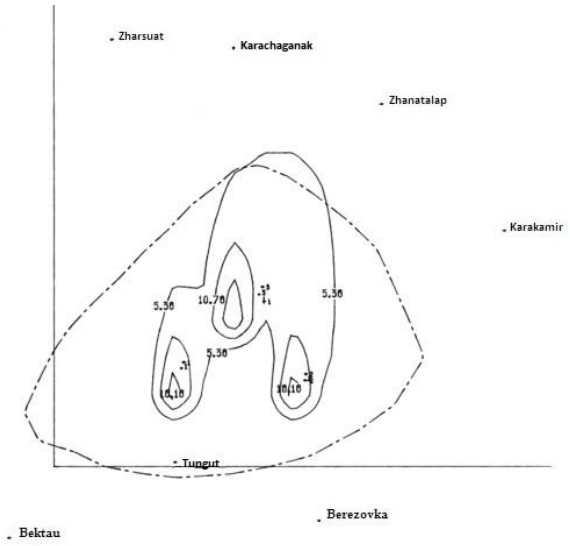

Fig. 3.5. Isolines of NO_2 concentrations in MAC shares at an altitude of 650 m.
Max NO_2 – 21.56

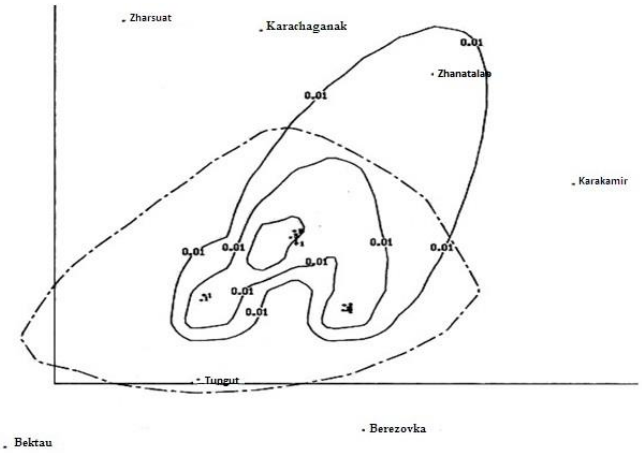

Fig. 3.6. Isolines of CO_2 concentration in the MAC shares at an altitude of 50 m.
Max CO_2 – 0.03

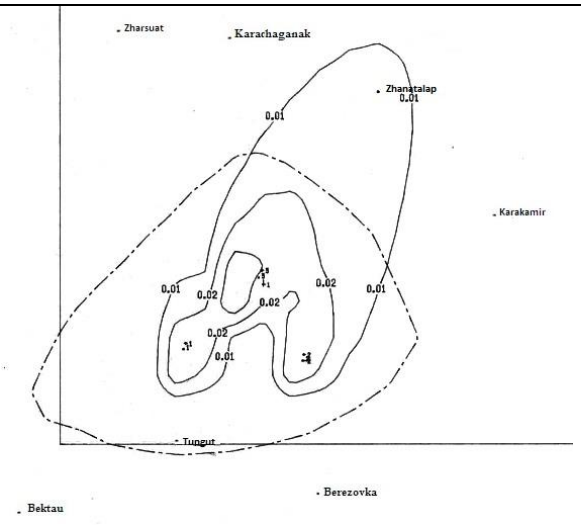

Fig. 3.7. Isolines of CO_2 concentration in the MAC shares at an altitude of 250 m.
Max CO_2 – 0.03

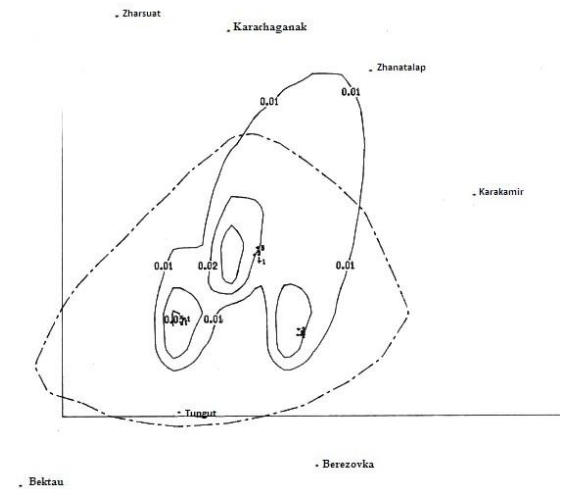

Fig. 3.8. Isolines of CO_2 concentration in the MAC shares at an altitude of 650 m.
Max CO_2 – 0.04

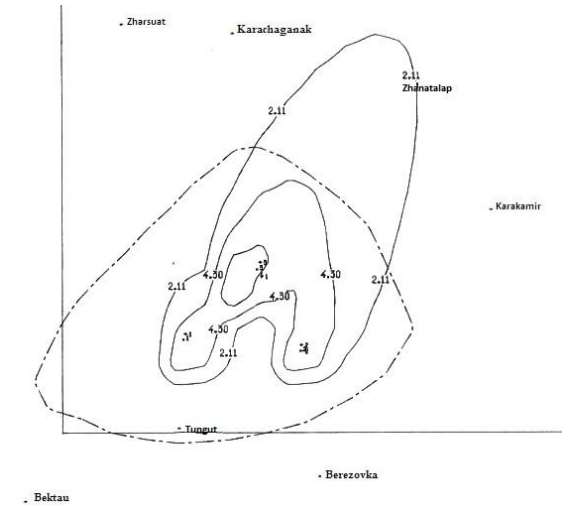

Fig. 3.9. Isolines of CO_2 concentration in the MAC shares at an altitude of 50 m.
Max CO_2 – 8.68.

The strongest source of pollution, as already noted, it is a unit UKSP-16. Additionally, these sources and have the highest effective emission height under these conditions of about 60 m. Therefore, as shown by Figures 3.5 and 3.11, this holds the greatest height exceeded MPC. For NO_2 MAC excess observed at all heights, including in the surface layer, several times. This is due to a large amount of impurities from the ejection units UKSP-16. The order volume of excess emission NO_2 compared with SO_2 value is close to 500.

The contribution of other sources of contamination to the total pollution is not so significant, and in addition, they have a relatively small effective height (within 50-100 meters). Of greatest interest is the distribution NO_2 in Figures 5.3-5.5. Admixture spread in the direction of movement of air masses, and because there is a rotation of the vector to the left velocity within the boundary layer of the atmosphere, the same orientation has the form of dispersion in different heights.

This is evident, for example, analysis of patterns 3.3- 3.5. The gas flow rate was taken as an input G_o=500 м^3/мин при заданном диаметре поперечного сечения d=20 sm. It is assumed that all wave processes accompanying the expiration of the initial stage has already ended, and the process is considered stationary phase jet expiration. Because of the uncertainties in the input data the percentage composition and physico-chemical properties of the condensate mixture, in this work (at 1st stage) was advisable to conduct parametric calculations of gas-dynamic fields flow in the stream corresponding to different initial conditions. The calculations were carried out in the framework of two-dimensional parabolized stationary Navier-Stokes equations using explicit numerical method of propulsion (Aidosov A.A., Aydosova G.A., Zaurbekov N.S., 2015; Godish Th., Davis W.T., Fu J.S., 2014).

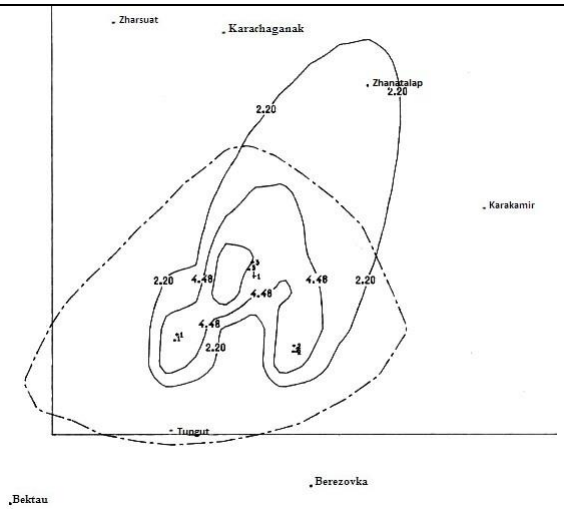

Fig.3.10. Isolines NO_2 concentrations in MAC shares at an altitude of 250 m.
Max NO_2 – 9.05

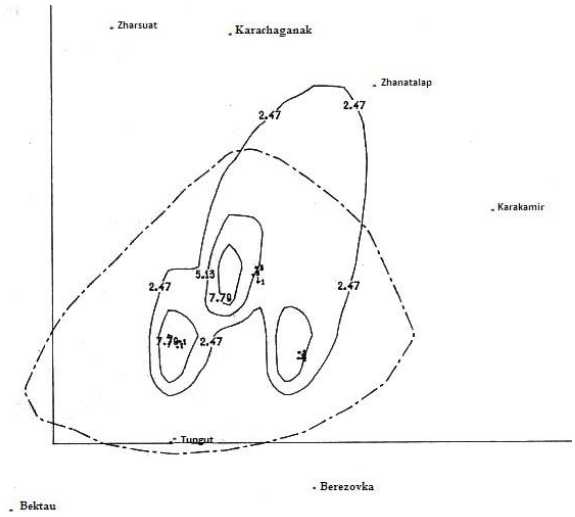

Fig.3.11. Isolines NO_2 concentrations in MAC shares at an altitude of 650 m.
Max NO_2 – 10.44

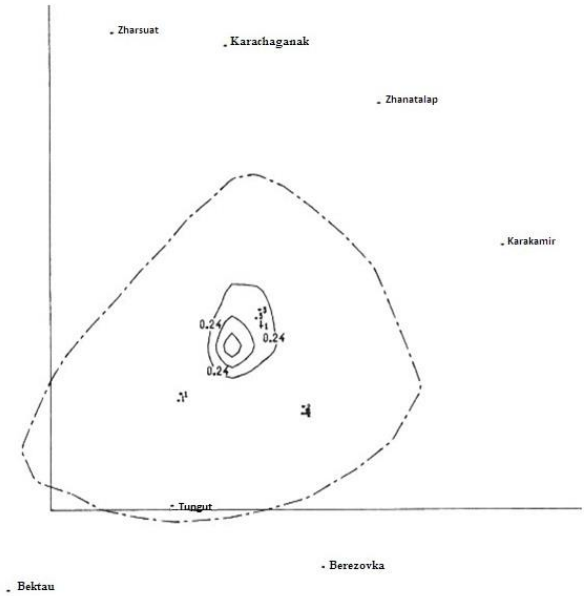

Fig. 3.12. Isolines SO_2 concentration in shares of MPC at a height of 50 m with convective conditions. The cross wind speed is 3 m/sec.

The jet was assumed axisymmetric, turbulent, isobaric. Physical and chemical processes include similar works. Here C-molar concentration of gas component flowing. atmosphere parameters: the composition-to-air; temperature – T-293,0^0 K; atmospheric pressure P_o=10^5 Pa; gas speed V_o=0 m/sec. In all cases the speed of calculations flowing from the gas well was assumed to be V_c=1060 m/sec.

Conclusion

As a result, the calculations showed that the kinematic (velocity) and geometric (vertical and horizontal) jet characteristics relatively weakly dependent on the thermodynamic and physico-chemical properties of the effluent from the well of the combustible mixture, from the initial temperature of the mixture composition. The calculation results show that the maximum height of lift gas flowing out of the well and the combustion products of the order H=200 m, with maximum horizontal dimensions of a jet containing products of burnt gases is less than 70 m. The maximum lifting height is determined by the condition that the vertical velocity of the burned gas in the jet was ~0,2%, of the gas velocity at the well cut, the latter at a given flow rate was V_c=1060 m/sec.

1. Aidosov A.A., Aidosov G.A., Zaurbekov N.S., (2010). *Models of the ecological environmental assessment under real atmospheric processes* – Almaty, 368 p.

2. Penenko V.V., Aloyan A.E. et al., (1985). *Modeling the impact of the characteristics of the Earth's surface changes on atmospheric processes in the boundary layer* – Meteorology and Hydrology – №5, p.45-53.

3. Yaglom A.M., (1972). *On turbulent diffusion in the atmospheric surface layer* – Math. USSR Academy of Sciences. Ser.: FAO. – (V.8) №6, pp. 579-593.

4. Aidosov A.A., Aydosova G.A., Zaurbekov N.S., (2015). *Model estimation of anthropogenic impact of the natural environment of oil and gas in the region components* – Almaty, monograph, p.160.

5. Aidosov A.A., Aydosova G.A., Zaurbekov N.S., (2010). *Models of the environmental situation of the environment under real atmospheric processes* – Almaty, 368 p.
6. Aidosov A., (2002). *Combined model for calculating the concentration of the non-stationary continuous source* – Hydrometeorology and ecology. Almaty, № 3, pp. 7-15.
7. Mickens. R.E., (2015). *Difference Equations: Theory, Applications and Advanced Topics, Third Edition*
8. Klapp J., Chavarría G.R., Ovando A.M., (2015). *Selected Topics of Computational and Experimental Fluid Mechanics*
9. Priti K.R., (2015). *Mathematical Models for Therapeutic Approaches to Control HIV Disease Transmission*
10. Friedman A., Kao Ch.-Y., (2014). *Mathematical Modeling of Biological Processes* – p.139
11. Gilbert K.M., Blossom S.J., (2014). *Trichloroethylene: Toxicity and Health Risks* – p.238
12. Alvarez M.A., (2014). *Plant Biotechnology for Health: From Secondary Metabolites to Molecular Farming*
13. Mansnerus E., (2014). *Modeling in Public Health Research: How Mathematical Techniques Keep Us Healthy*
14. Cojocaru M., Kotsireas I.S., Makarov R., Melnik R., Shodiev H., (2015). *Interdisciplinary Topics in Applied Mathematics, Modeling and Computational Science*
15. Cottrell M., (2014). *Guide to the LEED Green Associate* – V4 Exam, p.109
16. Bowden R., (2015). *Impact of Science and Technology: Energy Sources* – p.34
17. Fleming J.R., Johnson A., (2014). *Toxic Airs: Body, Place, Planet in Historical Perspective*
18. Walker C., (2014). *Ecotoxicology: Effects of Pollutants on the Natural Environment*
19. Amano R.S., Sundén B., (2014). *Aerodynamics of Wind Turbines: Emerging Topics* – p. 161
20. Couling S., (2015). *Measurement of Airborne Pollutants* – p.7
21. Syngellakis S., (2014). *Biomass to Biofuels* – p.55
22. El-Hinnawi E., Hashmi M.H., (2015). *The State of the Environment* – p.5
23. Garrett H., (2014). *Organic Lawn Care: Growing Grass the Natural Way* – p.12
24. Dr Marieke K., (2014). *Environmental Crime and its Victims: Perspectives within Green Criminology*
25. Steyn D., Mathur R., (2014). *Air Pollution Modeling and its Application XXIII* – p.155
26. Godish Th., Davis W.T., Fu J.S., (2014). *Air Quality, Fifth Edition* – p. 461
27. Mcevoy M., (2014). *External Components*
28. Klaassen C., Watkins J.B. III, (2015). *Casarett & Doull's Essentials of Toxicology, Third Edition*
29. Hemond H.F., Fechner E.J., (2014). *Chemical Fate and Transport in the Environment*
30. Nishii R., Ei Sh.-I., Koiso M., Hiroyuki O., Okada K., Saito Sh., Shirai T., (2014). *A Mathematical Approach to Research Problems of Science and Technology: Theoretical Basis and Developments in Mathematical Modeling*
31. De S., Hwang W., Kuhl E., (2014). *Multiscale Modeling in Biomechanics and Mechanobiology*
32. Kluever R.C., Kluever C.A., (2015). *Dynamic Systems: Modeling, Simulation, and Control*